

Explained and Unexplained Momentum Impulse Transfer Events (MITEs)

Dr. Michael Bantel

ExoAnalytic Solutions Inc.

Dr. Phillip Cunio, Dr. Douglas Hendrix, William Therien

ExoAnalytic Solutions Inc.

ABSTRACT

Precision orbit determination (OD) and characterization of resident space objects (RSOs) are fundamental components of Space Situational Awareness (SSA). Over 600 days beginning January 1, 2015, ExoAnalytic Solutions collected more than 60 million correlated astrometric measurements of active and inactive resident RSOs in geosynchronous Earth orbit (GEO) and in the near-GEO region using a global network of ground-based telescopes. Orbit Determination (OD) on several inactive RSOs in sub-synchronous (e.g., spent upper stages) and super-synchronous (e.g., retired satellites) orbits revealed occasional momentum impulse transfer events (MITEs) with detectable In-track velocity changes of 0.2 to 10 mm/s. These MITEs could not be explained using the accepted gravitational model and an isotropic spherical solar radiation acceleration. Two additional radiation pressure models were considered: a Yarkovsky effect and an asymmetric radiation pressure (diffuse ellipsoid), adding one and two additional free parameters to the model, respectively. Both models include a radiation pressure component perpendicular to the solar direction and in the RSO's orbital plane. The Yarkovsky and Ellipsoid radiation pressure, in combination with the RSO traversing the Earth's Umbra, can produce a measureable change in the RSO's mean motion; a Δv of 0.5 mm/s per season is not uncommon. OD was performed using the three radiation pressure models (Sphere, Yarkovsky, and Ellipsoid) on six inactive RSOs having 9,000 to 35,000 observations over 600 days. The Ellipsoid model was in good agreement with 95% of the observations falling within a window of ± 20 microradians, or approximately ± 0.8 km, over the entire 600 day duration, which included three equinox seasons. Data collection and analysis of inactive RSOs aids the SSA mission of precision tracking and characterization of debris in the space environment.

1. INTRODUCTION

With hundreds of days of data on hundreds of RSOs, it is possible to compare a detailed force model to the observations of inactive space objects. If the model and the observations are consistent, then the model provides a means to predict and characterize RSOs. If the model is found to be inconsistent with the observations, then there are additional unaccounted forces acting on an RSO which may or may not be understood. Using a force model to forward predict the state of an RSO or to detect changes, requires an understanding of the model's limitations. A single force model with as few free parameters as possible that is found to be consistent with observations of numerous inactive RSO over long durations and degrades gracefully is desirable. Such a model is a fundamental component for successful SSA.

By January 2015, the ExoAnalytic Space Operations Center (ESpOC) global network of ground-based telescopes was steadily collecting observations over the entire GEO belt. Prior to and during that year, numerical propagators and orbit determination programs were in development at ExoAnalytic and were tested on observations collected by the network. Analysis of ESpOC data was a key element in gaining confidence that the propagation model was physically correct. Using the ESpOC data, an error in the moon position model or an incorrect formulation of the stellar aberration correction could be observed via poor fits between observations and OD results (i.e., residuals that exceeded noise estimates). Active satellites with many observations, such as Galaxy 15, were analyzed; however, this was only valid over durations devoid of maneuvers, typically between 5 and 10 days. For OD testing using longer durations of ten or more days, the ideal RSO type is debris, which does not perform deliberate maneuvers.

At the end of 2015 inconsistencies were identified between the observations of inactive RSOs and the accepted gravitational model with an isotropic radiation pressure. In examining the in-track residuals between the fitted model and the observations, it appeared that there were times when the RSOs attained velocity changes on the order of 0.2 to 10.0 millimeters per second in the in-track direction. These small velocity changes were called Momentum Impulse Transfer Events (MITEs). Coincidentally, a typical dust mite is 0.2 -0.3 millimeters in length, comparable

to the distance change per second of some of the MITEs observed in this paper. While the velocity change (delta-v) of this magnitude may appear inconsequential, it is statistically significant and easily observed in the in-track residuals (predominantly the right ascension residual for circular low incline orbits) of the analysis when examining long observation durations (20 or more days).

The residuals referred to in this paper are the difference between the model's predicted line-of-site (LOS) and that measured. The angular difference unit used in this paper is the microradian--1 millionth of a radian--which is roughly 1/5 of an arcsecond (5 μ rad is approximately 1 arcsecond). At GEO ranges, one μ rad represents about 36 meters as viewed from Earth's surface. The reference frame used in the analysis is J2000, and the angular residuals are given in two directions, the Right Ascension (RA) and Declination (DEC). (One caveat: an Euler angle convention for defining angles was used in the J2000 for determining the residuals. The RA is unaltered; however, the DEC residual requires a sign change to be consistent with using an angle from the equatorial plane.) The structure and dispersion seen in the residuals provides insight to the model's limitations and the quality of the measurements. Because the models used in OD have between 7 and 9 free parameters, interpretation of the structure seen in the residuals is not always obvious; the true physical accelerations can be obfuscated or mitigated by the optimized fitting.

A velocity change in the in-track direction causes a change in an orbit's mean motion. When examining the residuals between an orbit that has an in-track delta velocity change compared to an orbit that has no velocity change, there will be an arc length difference along the orbit's path that grows approximately linear with time. The mean magnitude rate of change of the arc length difference between the two orbits is approximately negative 3 times delta-v. For example, after 50 days at a GEO radius the change in arc length between orbits due to one having a 1mm/sec delta-v is: $(3)(.001 \text{ m/s})(24 \times 3600 \times 50) = 13 \text{ km}$. At earth's surface, 13 km appears as a 360 μ rad deviation. This deviation is significant because it is persistent and is many times greater than the measurement uncertainty (1-5 μ rad). A velocity change in any particular direction causes an oscillation proportional in amplitude to the delta-v in its respective in-track or out-of-track direction. It is only the in-track direction aligned with the velocity that has a proportional drift that becomes increasing observable over time. To take advantage of detecting a small in-track velocity change, observations over several days need to be collected both before and after the event. The ESPOC dataset has full GEO coverage with over 600 nightly observations of numerous RSOs, which satisfies the data requirements to exploit this favorable in-track measurement scenario.

2. ANALYSIS OF SIX ROCKET BODIES

Orbit Determination (OD) using three different SRP acceleration models (Figure 1) was performed on six RSO rocket bodies (listed in Table 1).

Table 1: Six rocket bodies examined in this report. The estimated Area to Mass Ratio (AMR) is discussed later in the paper; the units are (m² per hecto kg or 100 kg). The Period, Inclination, Eccentricity, and Semi-Major Axis are evaluated at the midpoint of the observation data set on day 300 (Julian Date 2457323.0 or Oct 27, 2015 at 12:00 UTC).

NORAD ID	International Code	Name	Number of Observations	AMR (m ² /hkg)	Period (24 hours)	Inclination (deg)	Eccentricity
02222	1966-053J	TITAN 3C R/B	30043	0.693	0.9370550	1.38120	0.01625
03292	1968-050J	TITAN 3C R/B	33067	0.722	0.9470793	0.9895	0.01623
09998	1974-033F	SMS 1 AKM	9063	1.908	0.8606988	2.3754	0.02506
36359	2010-002B	BREEZE-M R/B	33558	0.868	0.9611243	4.3678	0.02134
39376	2013-062B	BREEZE-M R/B	34188	0.856	0.9595882	1.4372	0.02530
39614	2014-010C	BREEZE-M R/B	28688	0.766	1.1041027	1.2678	0.06840

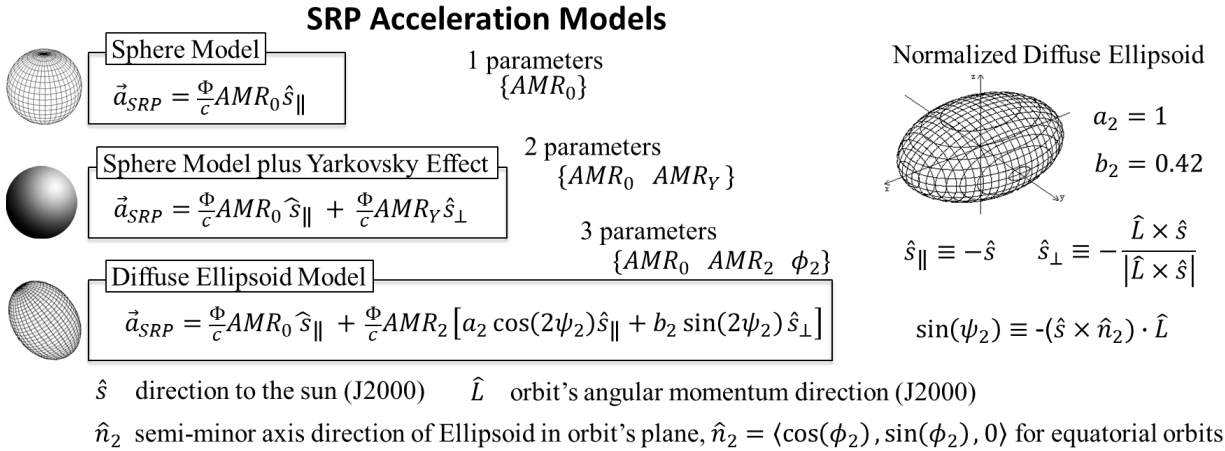


Fig. 1: These three SRP Acceleration Models, combined with the gravitational forces, were used in the propagation and OD of the six rocket bodies seen in Table 1 and for numerous figures to follow. A positive AMR_Y corresponds to an acceleration that increases the energy of the orbit (for an object orbiting the source).

2.1 Sphere Model

The first model used in the OD is a 7 parameter fit; 6 parameters for the state vector and 1 parameter for a spherical radiation pressure proportional model. The Sphere Model fits the data well over an 80-day period, as seen in figures 2 and 3, which has no Earth umbra crossings.

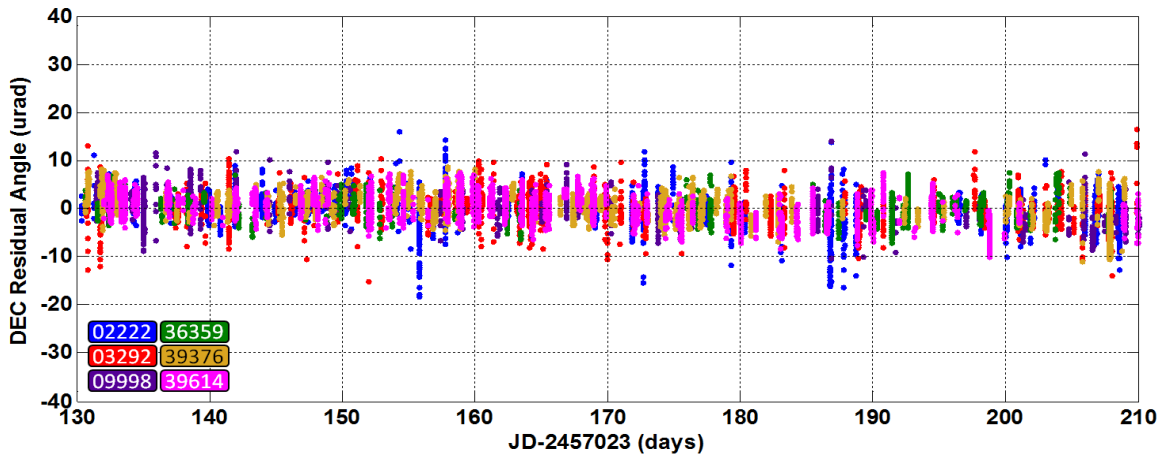


Fig. 2: Declination (DEC) residuals of an 80 day fit for six RSO rocket bodies. See Figure 3 for additional details.

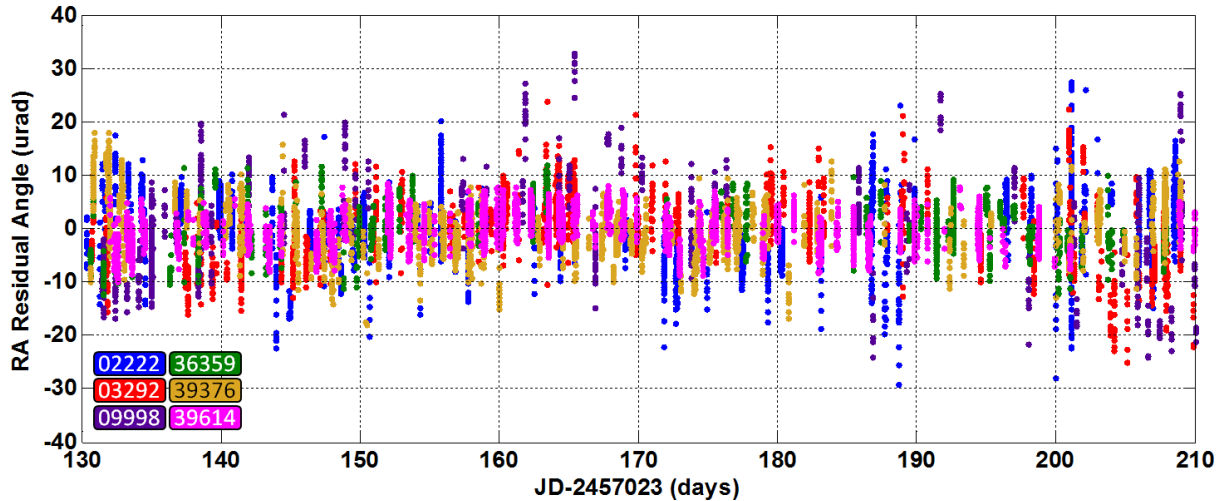


Fig. 3: Right Ascension (RA) residuals. The residuals are color coded according to the RSO being observed. This 7 parameter fit (State vector 6, SRP 1) is over an 80-day observation duration where the RSO does not traverse the Earth's umbra, May 10, 2015 to July 29, 2015. The RA and DEC residuals appear well-behaved.

The OD fit results, as seen in Figures 2 and 3, were then propagated over a 600-day duration, January 1, 2015 through August 22, 2016, and compared to ESpOC observations. The residuals are seen in Figures 4 and 5. Initially, when the analysis only included one equinox season, proposed physical explanations for observed MITEs included: thermally-induced agitation causing outgassing, low velocity debris collisions, meteorite collisions, and the like. However, since three equinox seasons have been observed, the sign and magnitude of the MITEs, as seen in RA residuals, are all suspiciously consistent each season for each RSO. Even the DEC residuals display a similar pattern. Additionally, the RA MITEs do not have sharp transitions as if due to a single impulse; rather, they appear to happen over time during the umbra transit season. Random events do not have this pattern; the evidence suggests that the 7 parameter force model lacks phenomenology associated with the RSO's traversing the Earth's umbra. The force model does include the umbra shadowing the RSOs; however, with or without this shadowing, the motion of the RSO does not change significantly. This is because during the time in the umbra the SRP that is effectively turned off is predominately in the radial direction and does not cause any significant change in the orbit's period.

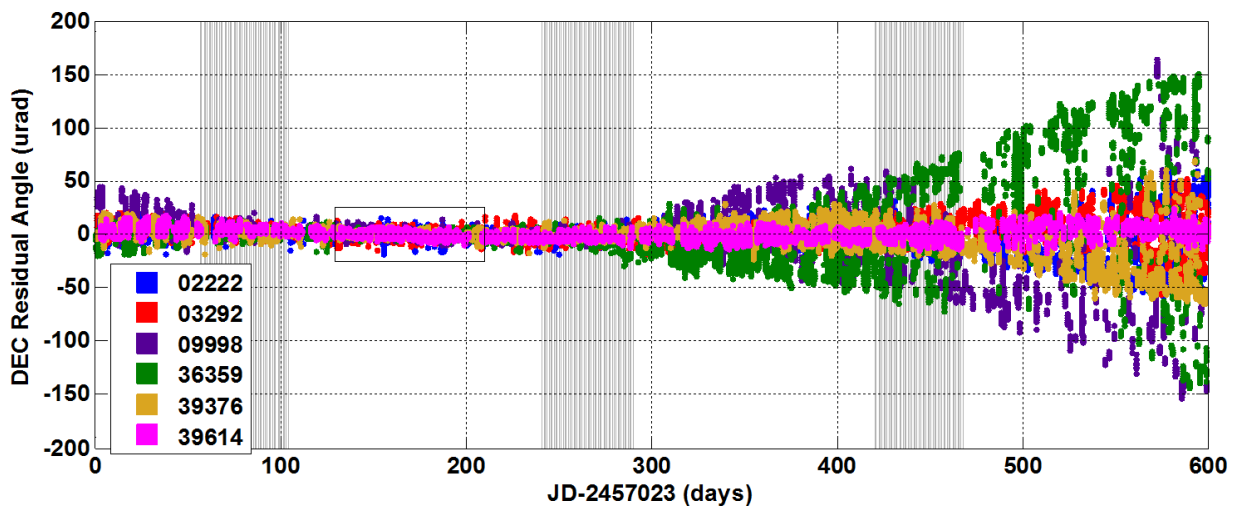


Fig. 4: Declination Residuals versus time. See Figure 5 for additional details.

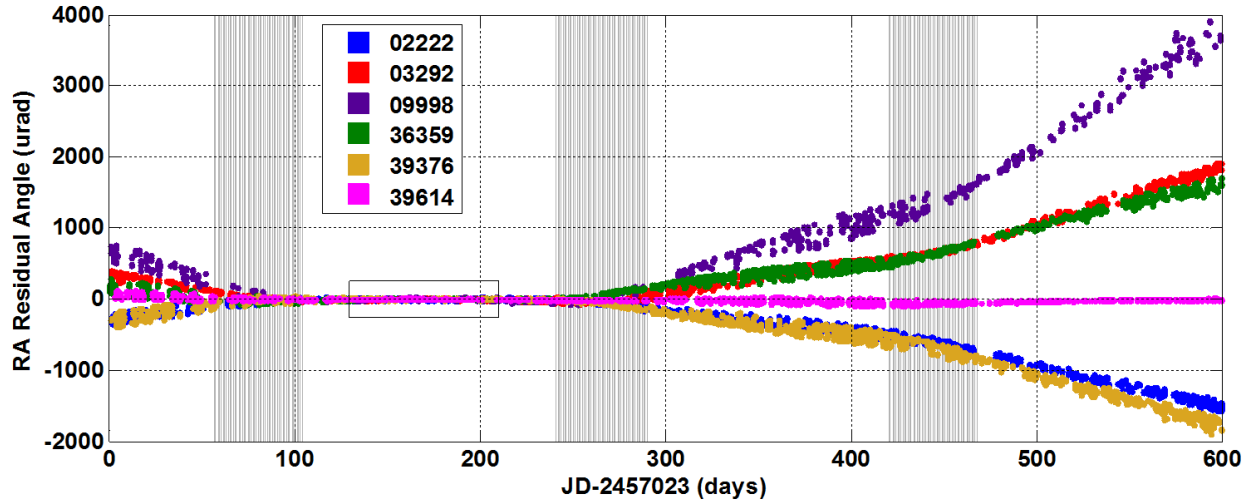


Fig. 5: RA residuals versus time. The parameter fit as seen in Figures 2 and 3 was propagated over 600 days and compared to the ESpOC observations. The black rectangle represents the 80-day fitting region. The vertical gray line groups centered at approximately 80, 275, and 440 days are the equinox seasons for RSO 03292, which are close, but not exactly the same as, the other RSOs' umbra transit seasons. A pattern can be seen in the RA slope change when passing through each equinox season.

2.2 Yarkovsky Model

From the residuals in Figure 5, it appears that during the equinox season, the RSO gets a positive or negative velocity bump in its in-track direction. For RSOs 2222, 3292, 36359, and 39367 the magnitude of a delta-v necessary to cause the change in slope each equinox season as seen in the plots is roughly 0.5 mm/s. During each season an RSO cumulatively spends approximately 2 days in the Earth's Umbra. A velocity change of 0.5 mm/s over 2 days corresponds to a uniform acceleration of approximately $3E-9 \text{ m/s}^2$. For an RSO with an effective AMR of $8E-3 \text{ m}^2/\text{kg}$ (or 125 kg per m^2), the radiation pressure acceleration is approximately $(1372)/(3E8)(8E-3) \approx 3.6E-8$. The missing acceleration needed to explain the MITEs seen during the equinox seasons is roughly 1/10 of the solar radiation acceleration of the RSOs.

If the solar radiation acceleration has a component perpendicular to the direction of the sun and lies in the orbital plane, then this acceleration (or lack thereof) can supply the missing acceleration necessary to remove the MITEs as seen in Figure 5. Two different physical mechanisms can provide a perpendicular SRP acceleration: the Yarkovsky effect [1] and the SRP of an asymmetric (non-spherical) object. Models for these two accelerations are shown in Figure 1.

The 7 parameter Sphere model can be extended to include one additional parameter representing a magnitude of a perpendicular SRP acceleration. This is the Yarkovsky model. A good fit to this model does not imply that the Yarkovsky effect is being observed; rather this is acknowledging that the Yarkovsky effect is a valid physical mechanism for the added term in the model. OD results using the Yarkovsky model are as seen in Figures 6 and 7.

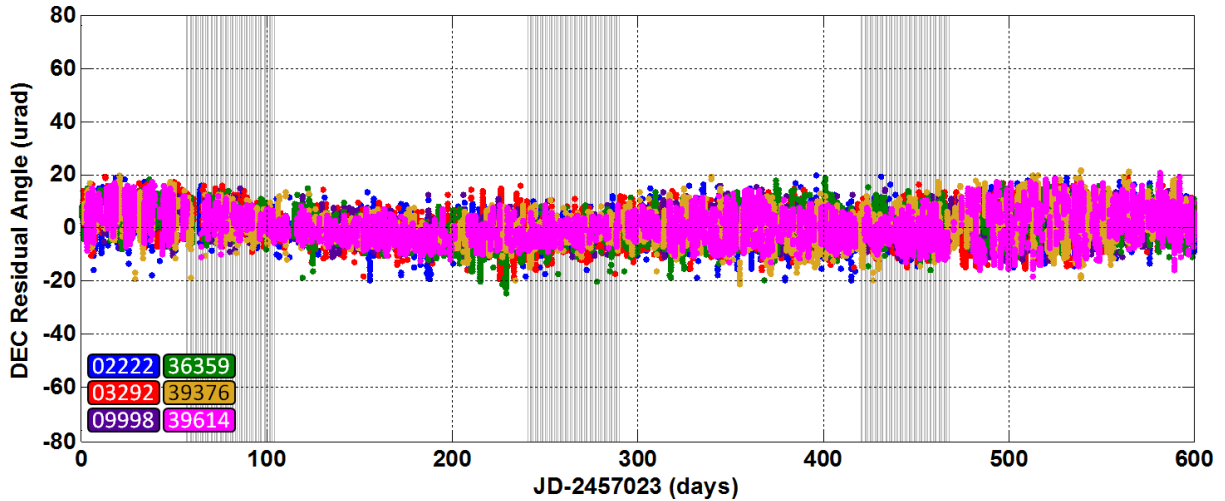


Fig. 6: Declination residuals using the 8 parameter Yarkovsky model. Notice the residuals are significantly reduced compared to Figure 4. Nearly 100% of the DEC residuals are within ± 20 microradians over the entire 600-day duration.

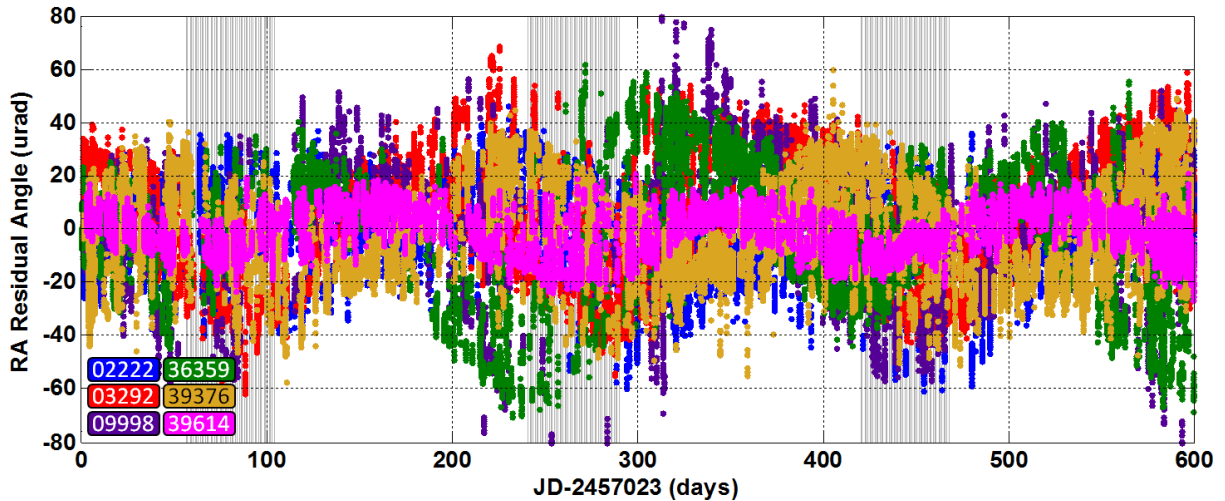


Fig. 7: RA residuals using the 8 parameter Yarkovsky model. Notice the residuals are significantly reduced compared to Figure 5 (i.e. the MITEs at the equinox causing the RA residuals to diverge are not seen).

The significantly reduced residuals due to the Yarkovsky model demonstrate that the MITEs seen in Figure 5 are likely artifacts of a naturally occurring umbra transit and an in-track perpendicular component associated with the SRP. The AMR parameter values used in the fit are shown in Table 2. Structure is still observed in the RA residuals that appear as a sinusoidal modulation period of approximately half a year. In Figure 8, the RA residuals are re-plotted but separated by $50 \mu\text{rad}$ for each RSO so that the individual sinusoidal trend in the residuals can be seen.

Table 2: Results of the Yarkovsky model for the OD using 600 days. AMR_0 is the standard spherical SRP parallel to the solar direction, AMR_Y is the Yarkovsky perpendicular magnitude in the orbital plane and is signed depending on direction. A positive sign is an acceleration in the direction $(\mathbf{S} \times \mathbf{L})$ where \mathbf{S} is the direction to the Sun and \mathbf{L} is the orbit's angular momentum vector. The angle θ_Y is the total SRP vector's angle from the $-\mathbf{S}$ direction. The standard deviation (STD) of the DEC and RA residuals are the last columns.

NORAD ID	Name	AMR ₀ (m ² /hkg)	AMR _γ (m ² /hkg)	θ _γ (deg)	STD of DEC Residuals (urad)	STD of RA Residuals (urad)
02222	TITAN 3C R/B	0.738	+0.057	+4.5	4.8	15.9
03292	TITAN 3C R/B	0.720	-0.071	-5.6	5.1	20.9
09998	SMS 1 AKM	1.786	-0.132	-4.2	5.0	27.2
36359	BREEZE-M R/B	0.809	-0.057	-4.1	4.5	22.1
39376	BREEZE-M R/B	0.866	+0.073	+4.8	5.4	18.1
39614	BREEZE-M R/B	0.776	-0.005	-0.4	6.0	7.5

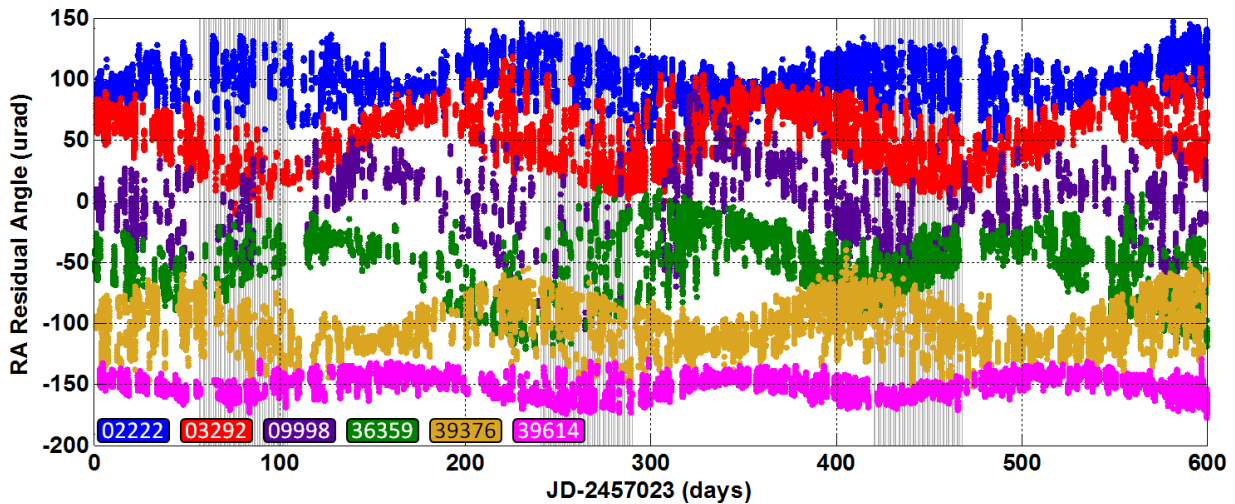


Fig. 8: RA residuals after OD using an 8 parameter Yarkovsky model. The RSOs are separated in increments of 50 μrad so that the RSO's residuals are less overlapped compared to that of Figure 7.

2.3 Ellipsoid Model

Another physical means for a perpendicular SRP to occur is if the RSO is non-spherical. A specular reflecting plate in space oriented with the normal vector not pointing at the sun source will have a perpendicular SRP component. Similarly, a diffusely reflecting ellipsoid with two different axes in the plane of the orbit will have a non-zero perpendicular SRP component. This is called the Ellipsoid model. Unlike the Yarkovsky model that has a constant perpendicular component (assuming the source flux is constant), the Ellipsoid model's perpendicular component has a dependency on the angle between the Ellipsoid's semi-minor in-track axis and the solar direction; which is angle $\Delta\phi_{SE}$. The SRP in the solar direction also has a dependency on $\Delta\phi_{SE}$. The Ellipsoid's in-track semi-major and semi-minor axes influence the magnitude of the asymmetric perpendicular component. Both the parallel and perpendicular SRP magnitudes make two sinusoidal cycles over the course of a year as the Sun travels around the object (in the object's frame). In a way, this diffuse Ellipsoid model is like an SRP quadrupole moment. The Ellipsoid model has three SRP parameters: the zeroth sphere moment AMR_0 , the quadrupole like moment AMR_2 , and the orientation of the quadrupole defined as the Ellipsoid's in-track semi-minor axis in J2000 specified as a single angle relative to a selected direction. This Ellipsoid model is specified in Figure 1. OD performed using this 9 parameter Ellipsoid model yields residuals as seen in Figures 9, 10, 11, and 12. Table 3 shows SRP parameters and standard deviations of the residuals.

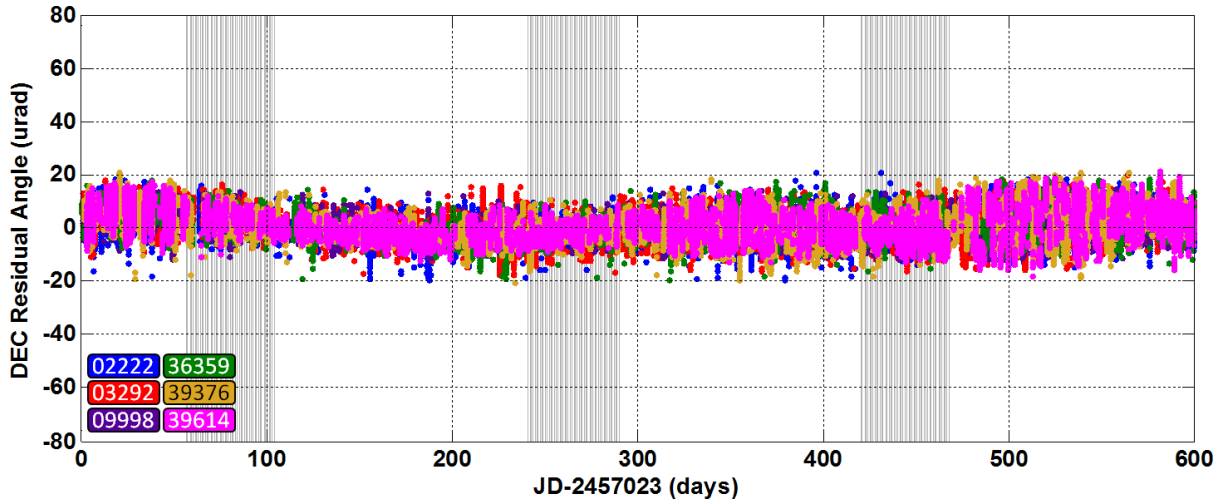


Fig. 9: DEC residuals of the Ellipsoid model over a 600-day fit.

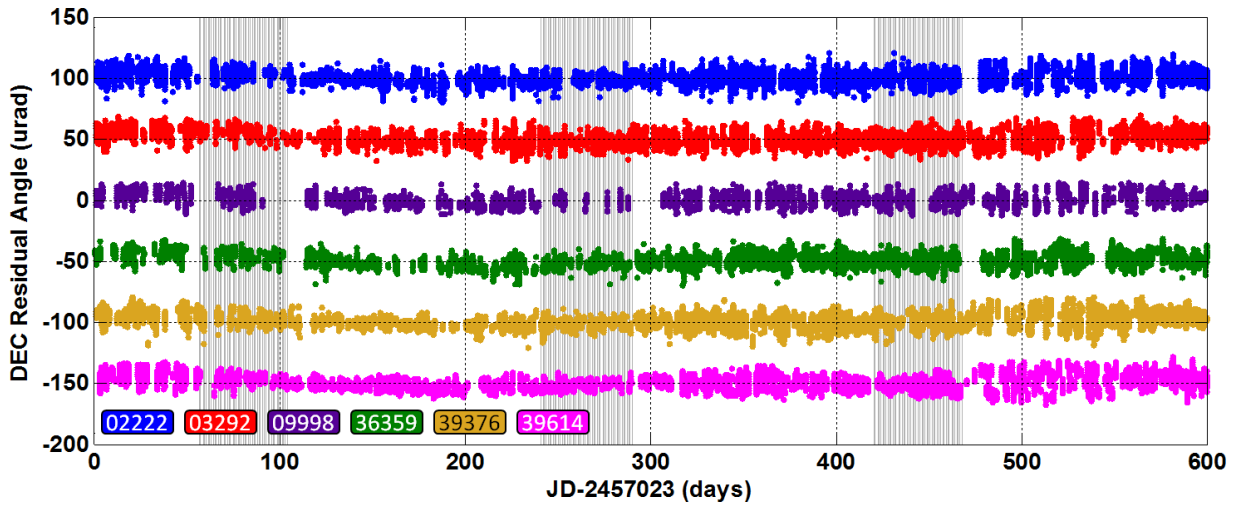


Fig. 10: DEC residuals of the Ellipsoid model offset in 50 μ rad increments to reduce overlap.

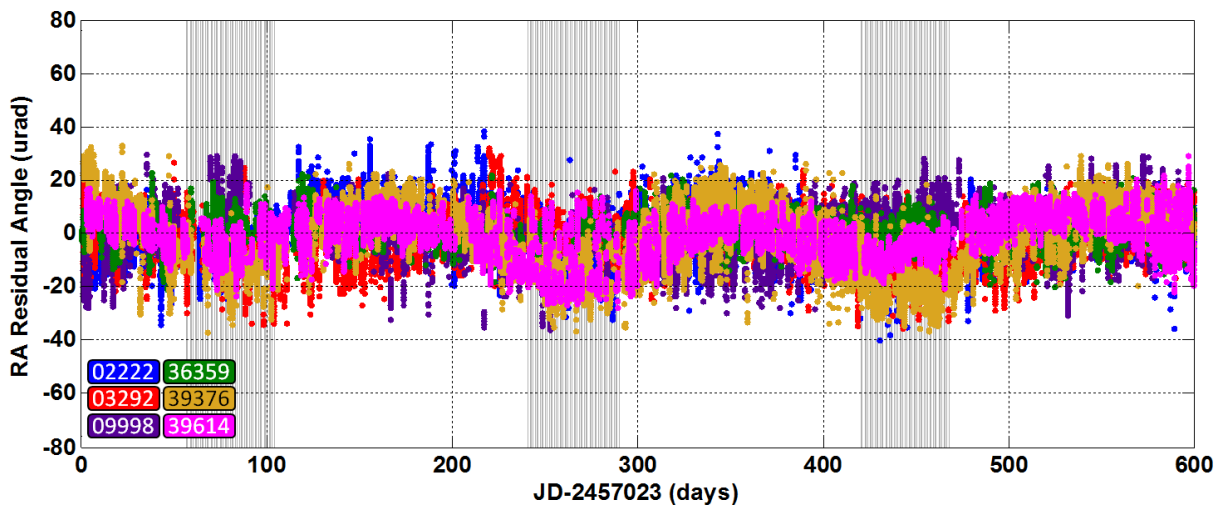


Fig. 11: RA residuals of the Ellipsoid model over a 600-day fit.

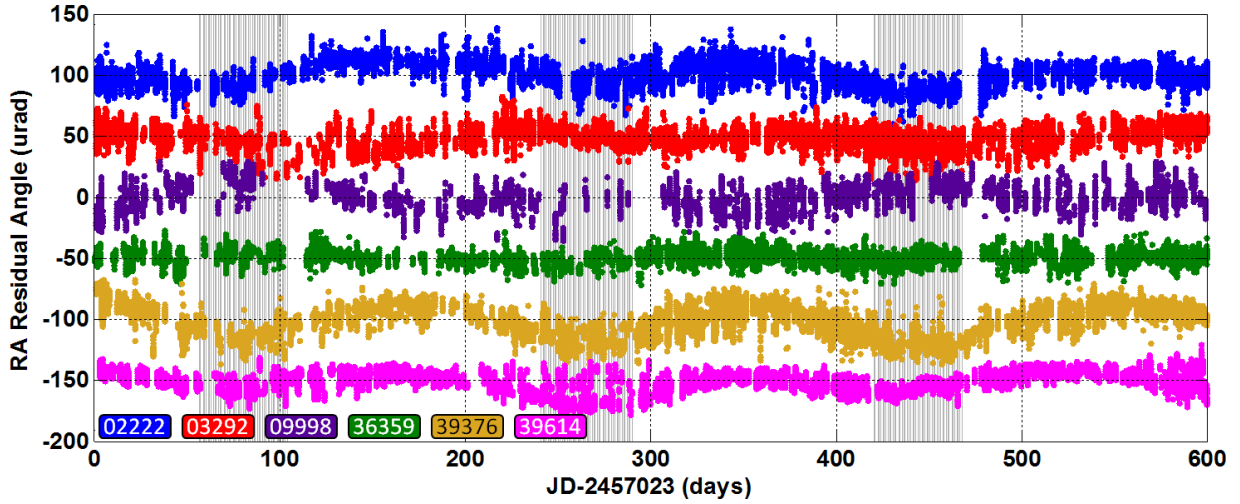


Fig. 12: RA residuals of the Ellipsoid model offset in 50 μrad increments to reduce overlap.

Table 3: Results of the Ellipsoid model for OD using 600 days. AMR_0 is the standard spherical SRP parallel to the solar direction, AMR_{AR} is the asymmetric quadrupole moment magnitude, and ϕ_{AR} is the orientation of the ellipsoids semi-minor axis ($-90 \leq \phi_{\text{AR}} \leq 90$) relative to the J2000 vernal equinox direction. A positive signed ϕ_{AR} is an acceleration in direction of $(\mathbf{S} \times \mathbf{L})$ where \mathbf{S} is the direction to the Sun and $\mathbf{L} = \mathbf{r} \times \mathbf{v}$ is the orbit's angular momentum vector. The standard deviation of the DEC and RA residuals are the last columns.

NORAD ID	Name	AMR_0 (m^2/hkg)	AMR_{AR} (m^2/hkg)	ϕ_{AR} (deg)	STD of DEC Residuals (urad)	STD of RA Residuals (urad)
02222	TITAN 3C R/B	0.693	0.161	+30	4.6	9.0
03292	TITAN 3C R/B	0.727	0.189	-37	5.1	6.7
09998	SMS 1 AKM	1.908	0.370	-53	4.6	10.1
36359	BREEZE-M R/B	0.868	0.197	-75	4.3	4.6
39376	BREEZE-M R/B	0.856	0.207	+30	5.3	11.9
39614	BREEZE-M R/B	0.766	0.015	-70	6.0	7.2

Note that the DEC residuals of the Yarkovsky model and Ellipsoid model are almost indistinguishable. However, the RA residuals of the Ellipsoid model are noticeably smaller than the Yarkovsky model as seen by STD of the RA residuals in Table 2 compared with Table 3.

The Ellipsoid model has an additional free parameter which aids in reducing residuals if the model's extra functional form is not orthogonal to the residual structure. The additional functional form that the Ellipsoid model has compared to the Yarkovsky model is a two-cycle modulation of the solar parallel SRP component over the course of a year. This effect is simply a physical consequence of using a diffusely reflective ellipsoid shape. In previous analyses not shown in this paper, OD using a sliding window width of 20 and 40 days, stepping in 5-day increments was applied to RSOs 2222 and 39614 using the 7-parameter Sphere model. A sinusoidal modulation with two cycles per year was clearly observed in the fitted AMR_0 over time for both RSO's.

The $[a_2, b_2]$ parameters seen in Figure 1 are not principle axis lengths of the Ellipsoid; they are the normalized modulation of the parallel and perpendicular radiation pressure acceleration for an illuminating source as the source goes 360 degrees around the Ellipsoid. Also, the Ellipsoid model represents the RSO's tumbled average shape; i.e. a double-sided precessing plate average is a bottomless cone. In the Ellipsoid model, the ratio between the semi-

major and semi-minor axes of the ellipsoid controls the relative magnitude of AMR_2 compared to AMR_0 . The values of a_2 and b_2 as shown in the Figure 1 formulas are [1, 0.42]. However, their ratio is not exactly constant over various relative principle axis length selections. Defining $a_2=1$, the value of b_2 will vary from [0.415 to 0.423] when the ratio of the minor/major axes length goes from 1 to 0.5 while the third out-of-plane Ellipsoid axis is set to the same length as the in-track major axis. When the minor axis is made smaller, the shape becomes more disk-like. Repeating this analysis and now letting the out-of-track axis equal the in-track minor axis, the b_2 value varies from [0.415 to 0.40] as the in-track axes ratio goes from 1 to 0.5. In this case, the shape looks more "rod"-like as the ratio gets smaller. Other shapes were examined, such as a stabilized double-sided diffuse plate, a stabilized double-sided specular plate, and a tumbling (end over end) averaged diffuse cylinder of different height to radius ratios. For these shapes, the parallel and perpendicular components of the SRP were examined as the source moved 360 degrees around the object. Higher harmonics beyond the quadrupole and a wider range of ratios between a_2 and b_2 parameters were observed.

2.4 SRP Model Comparisons

A comparison of the fitted AMR values is seen in Table 4.

Table 4: Comparison of the AMR values from the three models. Note the Sphere Model only used 80 days of observations from day 130 to day 210. The AMR for the perpendicular component of the SRP (AMR_{\perp}) at the time of the equinox for the Ellipsoid Model is the last column. The acceleration magnitude using the AMR is approximately $(1372)/(3E8)(AMR)$. The units for the AMR values shown are m^2 per 100 kg.

NORAD ID	Name	AMR ₀ (m ² /hkg)			AMR _⊥ (m ² /hkg)	
		Sphere (130-210)	Yarkovski (0-600)	Ellipsoid (0-600)	Yarkovski	Ellipsoid @ equinox
02222	TITAN 3C R/B	0.651	0.738	0.693	+0.057	+0.059
03292	TITAN 3C R/B	0.619	0.720	0.727	-0.071	-0.076
09998	SMS 1 AKM	1.921	1.786	1.908	-0.132	-0.149
36359	BREEZE-M R/B	0.959	0.809	0.868	-0.057	-0.041
39376	BREEZE-M R/B	0.757	0.866	0.856	+0.073	+0.075
39614	BREEZE-M R/B	0.851	0.776	0.766	-0.005	-0.004

3. UNEXPLAINED MITES

Not all rocket bodies fitted well to the Ellipsoid model. Some inactive RSOs had several MITES over the 600 days, while others only had one (or two), such as the Breeze-M rocket body with a 2,040 kg Dummy Sat 2 (NORAD ID 40355, International Code 2014-085A). OD fits of 40355 observations was done individually to the left and right of the MITE; specifically, to the left is a fit for day (10 to 125) and to the right is a fit for day (200 to 600). The MITE is seen in Figure 13.

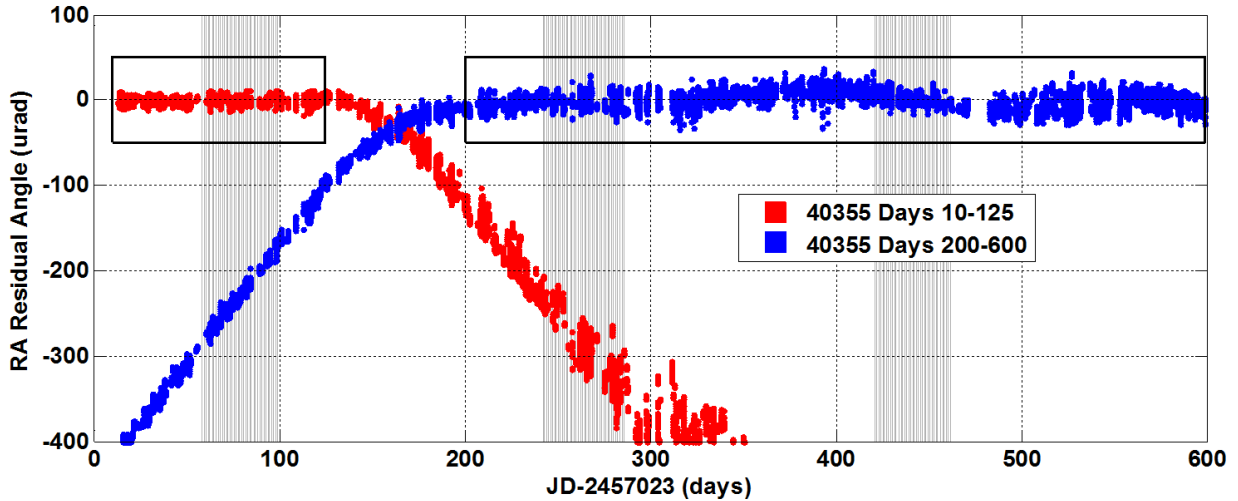


Fig. 13: RA residuals of 40355 using two different fitting regions as seen in the red and blue residuals. The black box shows the regions being fitted. The slope of the MITE is about $2.6 \mu\text{rad}/\text{day}$, indicating a Δv in the in-track direction of roughly $0.36 \text{ mm}/\text{sec}$.

The region of the MITE is not near an equinox transit nor does it fall in the shadow of the moon. Upon closer inspection, the MITE does not appear as a single impulse; rather, there appear to be a discrete few. Figure 14 shows the residuals over two different sections of the data.

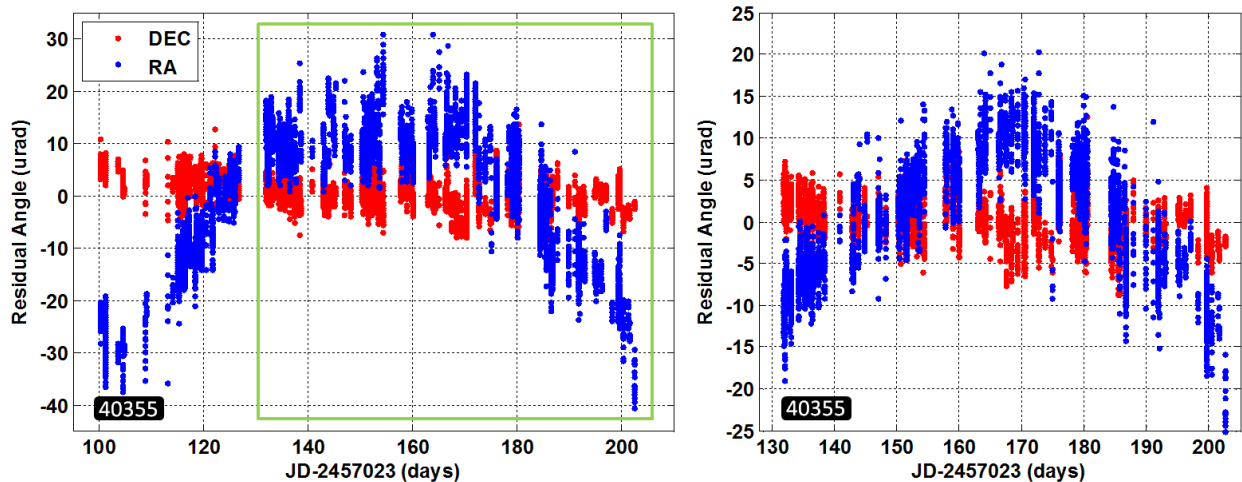


Fig. 14: The left and right plots are the residuals of an OD on observations of 40355 during the unexplained MITE seen in Figure 13. The left plot uses the observations from day 100 to day 210; the right plot uses observations from day 130 to 205. The red points are the DEC residuals, blue points are the RA residuals. The green box shows observations used in the right plot to isolate what appears to be a short single impulse MITE.

In the left plot of Figure 14 there appear to be two MITEs occurring at roughly day 130 and day 170. There could also be more subtle MITEs present that are obscured in the noise. The change in RA slope before and after the MITE suggest a Δv of $\sim 0.18 \text{ mm}/\text{s}$. Characterization of this MITEs Δv vector can be estimated assuming a single short impulse; however, the estimate depends upon the time of the impulse, which is not well known, having an uncertainty of a quarter of a cycle.

Another example of an unexplained MITE is from COSMOS 2479 (NORAD ID 38101 International Code 2012-012A). This is an inactive satellite [2] but at approximately 28-Sep-2015 06:35 UTC (JD:2457293.774 Day: 270.774) a MITE occurred, as seen in Figure 15.

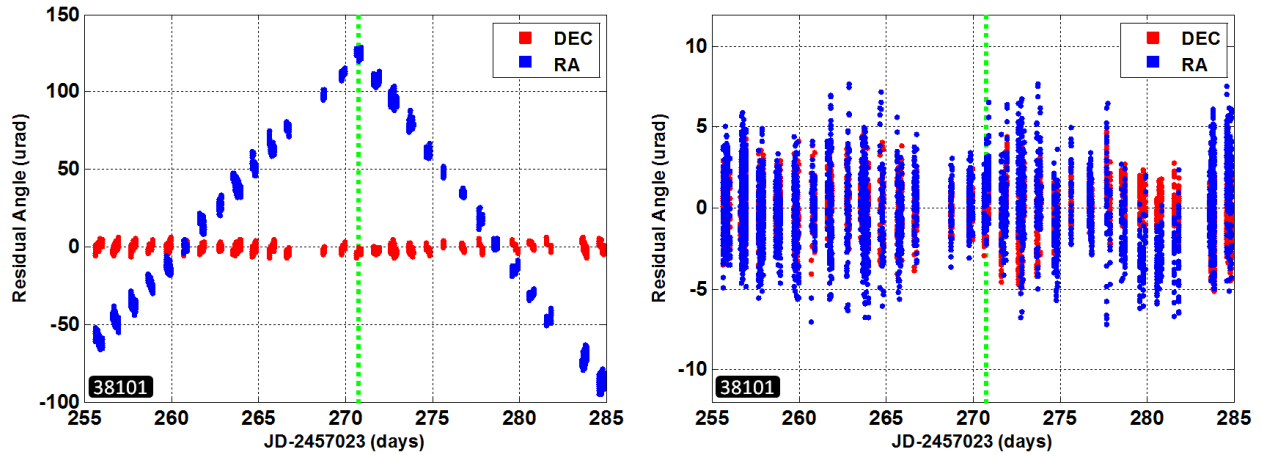


Fig. 15: Residual OD fits of RSO 38101. The left plot is the residual a 7 parameter OD over 30 days of observations. The right plot is a 10 parameter OD of the same data but has a separately fitted velocity to the left and right of day 270.774 indicated by the green dashed line.

The velocity difference between the before and after velocity at day 270.774 is $[-9.9, 16.3, 4.0]$ mm/s for radial, out-of-track, and in-track directions. This before and after velocity difference is an estimate of the MITE's delta-v. Defining the uncertainties of the MITE's delta-v requires incorporating the uncertainty of the time of the MITE and other factors. The OD of the MITE at a given time also includes a 9×9 covariance of the parameters [position, velocity before, and velocity after]. Performing this OD analysis over a grid of probable MITE times and evaluating χ^2 at each time allows the estimation of a probability distribution function (PDF) for the MITE time using the χ^2 values. Then a weighted average over time of the MITE's delta-v PDF can be evaluated using the MITE time PDF as the weight. However, sensitivity to the data span used, how observation outliers are handled, and/or how the observations are weighted can influence the results of the MITE's delta-v; and thus such factors also contribute to the delta-v uncertainty. These details are beyond the scope of this paper.

4. ANALYSIS DETAILS

4.1 Data Filtering

Raw observations are associated to an RSO using tracks from Space-Track[3]. These observations then pass through several filters where approximately 10% to 20% of the original observations are rejected in one of two ways. First, single observations in a timeframe window less than ± 40 seconds are rejected. Second, outliers are rejected based upon a smooth fit using the same night and sensor that are above 3 standard deviations of the residuals. Missed associations off by hundreds of microradians or other outliers from image co-processing with nearby stars, were removed by thresholding with a human-in-the-loop, accounting for an additional 2% - 5% of the observations' being rejected. Care was taken in the filtering processes to not reject observations unless there was reasonable confirmation that the observation was corrupted. In the residual plots, there remain a few noticeable outliers, but these points have minimal impact on results.

4.2 Acceleration Model

- Earth Gravitational Model: WGS84 model with EGM2008 coefficients through $n=8$. [4]
- Earth Orientation in J2000: Orientation is calculated using International Astronomical Union's Standards of Fundamental Astronomy (SOFA) software [5] and data tables [6].
- Moon and Sun Gravity: Uses the Moon and Sun position model found in "Constrained Admissible Region Multiple Hypothesis Filter" (CAR-MHF).
- Solar flux: Solar Flux at Earth's mean location from the sun is assumed to be 1372.5 W/m^2 and is normalized using the Sun's mean Range to Object to Sun Range.

- Earth's Albedo and Earth shine: The SRP of the Earth source is included. The Albedo is 0.306 and the Earth shine is 237 W/m^2 at Earth's surface. Both are assumed to be Lambertian Spheres.
- Solar Shadowing: The Earth and Moon eclipsing of the Sun use eclipsing circle equations in angular space.
- Not include: Drag, Solid tides, other planets, other smaller forces

4.3 Numerical Propagation and Orbit Determination

- Method: 4th order Runge-Kutta for 2nd Order Differential Equations.
- Maximum allowed step size is made proportional to $|x|/|v|$. About 500 steps per orbit are used for nominally circular orbits corresponding to the maximum step size of $|x|/|v|/80$.
- The Runge-Kutta is effectively seeded with the $-1/r^2$ solution. This enables the time step to be increased by a factor of 7 while still maintaining the same numerical precision as propagation without this approach based upon tests done near GEO orbits.
- Orbit Propagation is in C/C++ and MEX wrapped for use in MatLab.
- The time to propagate a nominal GEO orbit for a year is under 10 seconds.

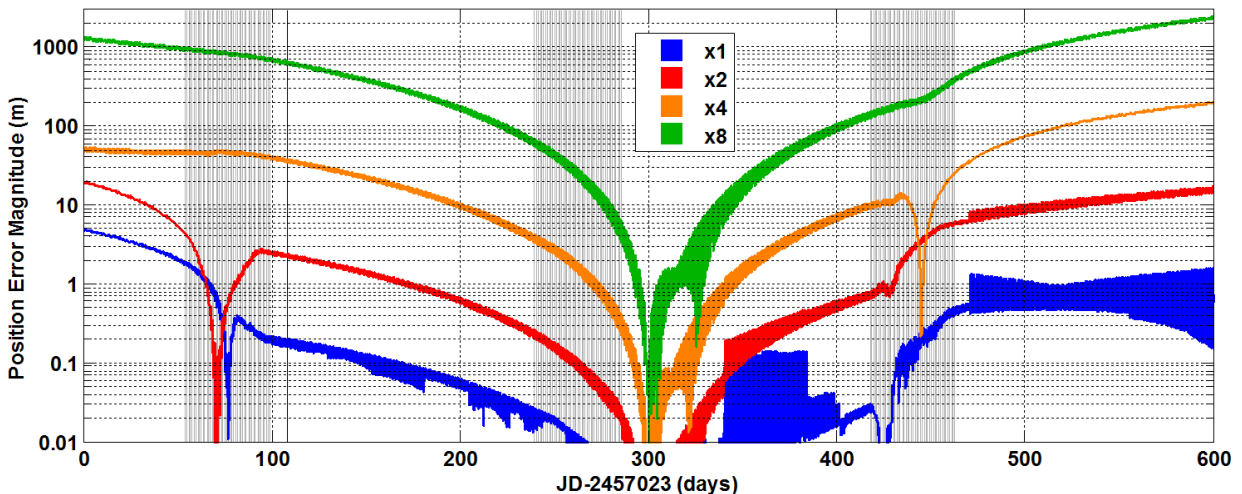


Fig. 16: A plot of position difference due to time step size for the numerical propagation of RSO 39367. The reference time step is $|x|/|v|/160 \approx 87$ seconds or about 1000 steps per revolution. The analysis in this paper used a time step of $|x|/|v|/80 \approx 174$ sec or about 500 steps per revolution. The difference is seen in blue. The time step was increased by a factor 2, 4 and 8 times {red, orange, green}.

The other RSOs showed a similar behavior to that seen in Figure 16. The largest difference of all RSOs examined for the operational time step as seen in blue was 40 meters, which corresponds to an angle less than $1.2 \mu\text{rad}$ at GEO distances. The OD fit parameters were evaluated at the center time of the dataset explaining the minimal differences seen at day 300. Small "glitches" seen on days {70, 77, 340, 427, 445, 471} are likely due to numerical error in seeding the Runge-Kutta. Propagation time at 500 steps per revolution for the 600 days was less than 13 seconds.

Orbit Determination Information:

- All observations are equally weighted.
- The fitted OD parameter set is the set that minimizes the sum of the residuals squared. This is a non-linear Least Squares Fit (LSF) of the observations.
- The seven parameter fit for the state and AMR_0 is automated. The fits for the additional one and two parameters of the Yarkovsky and Ellipsoid Models were performed by manual bracketing.

4.4 Observation Conditioning and Collection

- Stellar Aberration Correction: Corrected using CAR-MHF's Solar Position Model. Correction also includes the velocity due to the Earth's rotation.

- Sensor Location: Calculated in J2000 using the International Astronomical Union's Standards of Fundamental Astronomy (SOFA) software and data tables.
- Leap Second: Exception is handled for the end of June 2015 leap second.
- Shutter Delay: Observation times are corrected using an inferred static delay time for each unique sensor.

The ESPOC network has sites at various locations on Earth, as seen in Figure 17. Each unique RSOs observations in this paper are plotted in Figure 18 in apparent GEO Latitude vs. GEO Longitude space, highlighting the measurements taken across the network. These RSOs circle the fixed Earth every 6 to 26 days (being slightly sub or super GEO) and are seen by the entire network with over 100 sensors. Figure 19 shows RA residuals color-coded according to sensor.



Fig. 17: ExoAnalytic Global Sensor Network Site Footprint.

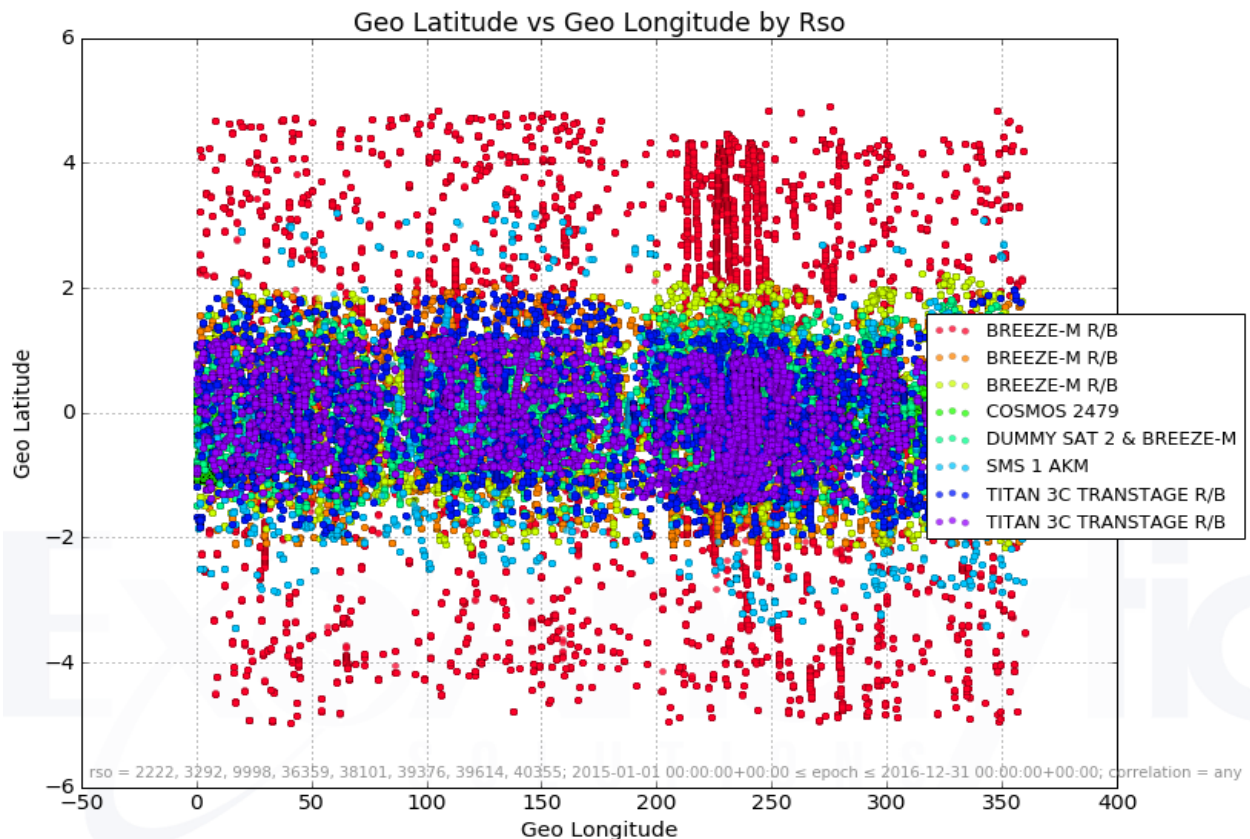


Fig. 18: Plot of all associated observations collected for the 8 subject RSOs during the 600 day study period. Angles are in degrees. Plot was generated by ExoAnalytic's *SpaceFront* which archives and enables queries with basic visualization of observations.

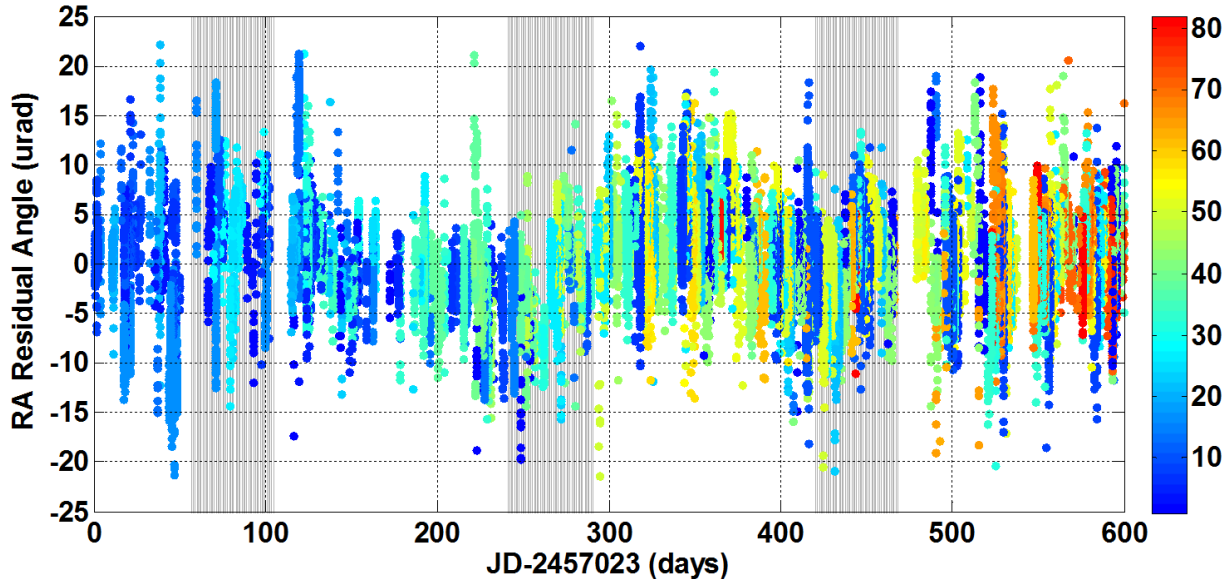


Fig. 19: RA residuals of the Ellipsoid model for RSO 36359 are color-coded according to the sensor that made the observation. This Breeze rocket body was seen by 80+ sensors as it circled the fixed earth once every 26.5 days. The revisit periodicity is mildly seen. The observation rate increase and new sensors coming online throughout the 600 days since Jan 2015 can also be slightly perceived. The RA residuals for this particular RSO are relatively small; the y axis at this range represents less than ± 1 km.

5. CONCLUSIONS

Orbit Determination (OD) on rocket bodies (excluding 40355) over a 600-day period had angular RA and DEC residuals corresponding to no more than ± 1 km, with standard deviations of these residuals ranging from 200 to 500 meters. The OD model employed 9 parameters; 6 for the state vector and 3 parameters characterizing the solar radiation pressure (SRP) that includes an area to mass ratio (AMR) and an in-track asymmetry magnitude and orientation. The analysis provides information about an RSO's AMR and enables high fidelity tracking, which is useful for Space Situational Awareness.

6. REFERENCES

1. Bottke, Jr., William F.; et al. (2006). "*The Yarkovsky and YORP Effects: Implications for Asteroid Dynamics*". *Annu. Rev. Earth Planet. Sci.* **34**: 157–191.
2. http://russianforces.org/blog/2014/06/russia_loses_its_only_geostati.shtml
3. www.space-track.org
4. Pavlis, N. K., S. A. Holmes, S. C. Kenyon, and J. K. Factor (2008), An Earth gravitational model to degree 2160: EGM2008, paper presented at the 2008 General Assembly of the European Geosciences Union, Vienna, Austria, 13–18 April 2008.
5. IAU OOFA Board, "*IAU SOFA Software Collection*", Issue 2016-05-03.
6. <https://www.iers.org/IERS/EN/Publications/Bulletins/bulletins.html>